A Journal of the Gesellschaft Deutscher Chemiker

Angewandte International Edition GDCh Chemie

www.angewandte.org

Accepted Article

Title: Fluorogenic Ag+-Tetrazolate Aggregation Enables Novel and Efficient Fluorescent Biological Silver Staining

Authors: sheng xie, Alex Y. H. Wong, Ryan T. K. Kwok, Ying Li, Huifang Su, Jacky W. Y. Lam, Sijie Chen, and Ben Zhong Tang

To be cited as: *Angew. Chem. Int. Ed.* 10.1002/anie.201801653
Angew. Chem. 10.1002/ange.201801653

Link to VoR: http://dx.doi.org/10.1002/anie.201801653
http://dx.doi.org/10.1002/ange.201801653

WILEY-VCH

10.1002/anie.201801653

WILEY-VCH

COMMUNICATION

Fluorogenic Ag^+-Tetrazolate Aggregation Enables Novel and Efficient Fluorescent Biological Silver Staining

Sheng Xie,[a, b] Alex Y. H. Wong,[b] Ryan T. K. Kwok,[a] Ying Li,[a] Huifang Su,[a] Jacky W. Y. Lam,[a] Sijie Chen*[b] and Ben Zhong Tang*[a, c]

Abstract: Silver staining, exploiting the special bioaffinity and the chromogenic reduction of silver ions, is an indispensable visualization method in biology. It is a most popular method for in-gel protein detection. However, it has been challenged with run-to-run viability, background staining, inability for protein quantification and limited compatibility with mass spectroscopic (MS) analysis, which are largely attributed to the tricky chromogenic visualization. Here, we reported a novel water-soluble fluorogenic Ag^+ probe, whose sensing is based on an aggregation-induced emission (AIE) process driven by tetrazolate-Ag^+ interactions. The fluorogenic sensing can substitute the chromogenic reaction, leading to a new silver fluorescence staining method. This new staining method offers sensitive detection of total proteins in polyacrylamide gel with broad linear dynamic range and robust operations that rival silver nitrate stain and the best fluorescent stain.

It has long been known that a number of biological structures are argyrophilic (silver loving). The utility of silver stains for biological applications dates back to 1800s. Largely by the silver-based Golgi's method, Camillo Golgi and Santiago Cajal were able to elucidate many aspects of the nervous system and for the contribution they received the 1906 Nobel Prize in Physiology or Medicine.[1] Silver staining is now an indispensable visualization method in biology and has established wide applications in histological characterization,[2] diagnostic microbiology,[3] karyotype analysis,[4] genomic[5] and proteomic[6] research. When used for the detection of proteins after electrophoresis, silver stain can detect a wide range of proteins and provides about 10-100 times better sensitivity than the classic Coomassie Brilliant Blue stain. Its working rationale is general. Silver ions bind to biological targets through interactions with carboxyl, amine, thiol and other electron-rich chemical groups.[7] The detection is then achieved by reducing the silver ions into metallic silver grains, which collectively label the sample with a dark color (Fig. 1a). Since the reduction varies at the site of proteins and has no clear end points, the silver grains formed usually have a broad range of sizes, leading to varied colors in the stained proteins. As a result, the colorimetric silver stains show poor linear relationship for protein quantification. Because of the tricky reduction, silver staining is also subjected to run-to-run variations and restricted to timing procedures for a good quality control.[8] To achieve the highest sensitivity in silver stains, glutaraldehyde is frequently used in an additional sensitization step to saturate silver species on proteins; meanwhile it cross-links proteins covalently, leading to challenges in downstream mass spectroscopic (MS) analysis.[6a] Omission of the glutaraldehyde enhances MS compatibility of silver stains while drastically decreasing their detection performance. The dilemma situation ultimately attributes to the chromogenic visualization in conventional silver stains.

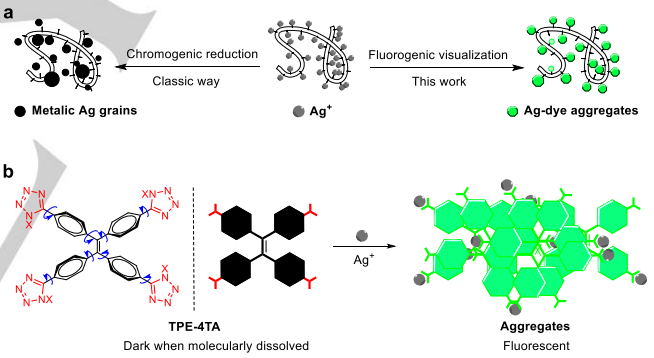

Figure 1. (a) The classic chrome-silver visualization (left) and hereby proposed fluorogenic visualization (right) of proteins. (b) **TPE-4TA** and the Ag^+ detection via a Ag^+-tetrazolate aggregation-triggered AIE process. *X* can be either H or Na^+. The possible tautomer 2*X*-tetrazole structure (in red) is not showed for clarity.

We envisioned that a fluorogenic visualization of silver ions, being an alternative to the chromogenic step (Fig. 1a), may relieve above-mentioned concerns from the reduction step and rejuvenate the traditional silver staining method. Considering fluorescent detection is fast and much more sensitive than absorption-based method, the strategy is furthermore plausible for developing new staining method with exceptional sensitivity. Though being straightforward, no fluorescent silver stains have been reported so far. The challenge might be that this method relies on a Ag^+-specific dye which can be finely tailed for the staining in complex environments (e.g. in a gel). On viewing of the *in situ* grain formation in silver stains, the dye is preferably able to settle down spontaneously upon Ag^+ recognition in gel, lighting up the target with a high signal to noise ratio.

[a] Dr S. Xie, Dr. R. T. K. Kwok, Dr. Y. Li, Dr. H. Su, Dr. J. W. Y. Lam, Prof. Dr. B. Z. Tang
Department of Chemistry, Hong Kong Branch of Chinese National Engineering Research Center for Tissue Restoration and Reconstruction, Institute of Molecular Functional Materials, State Key Laboratory of Neuroscience, Division of Biomedical Engineering, and Division of Life Science.The Hong Kong University of Science and Technology, Kowloon, Hong Kong, China.
E-mail: tangbenz@ust.hk

[b] Dr. S. Xie, A. Y. H. Wong, Prof. Dr. S. Chen
Ming Wai Lau Centre for Reparative Medicine, Karolinska Institutet, Hong Kong, China.
E-mail: sijie.chen@ki.se

[c] Prof. Dr. B. Z. Tang
Guangdong Provincial Key Laboratory of Brain Science, Disease and Drug Development, HKUST-Shenzhen Research Institute, Nanshan, Shenzhen, China.
Guangdong Innovative Research Team, SCUT-HKUST Joint Research Laboratory, State Key Laboratory of Luminescent Materials and Devices, South China University of Technology, Guangzhou, China.

Supporting information for this article is given via a link at the end of the document. ((Please delete this text if not appropriate))

10.1002/anie.201801653

COMMUNICATION

Inspired by the aggregation-induced emission (AIE) phenomenon,[9] the desired fluorogenic Ag^+ detection accompanied by an aggregation process, can be rationally achieved. Unlike conventional dyes, a typical AIE dye has a flexible structure and emits faintly when molecularly dissolved. In the aggregated state, the dye emits strongly. The fluorescence in responses to molecular states has been explored as a general way to design fluorogenic probes for metal ions, small molecules and enzymes.[10] In this work, we designed a tetrazole-tagged AIE luminogen, **TPE-4TA**, to sense Ag^+ in a fluorogenic manner. Many 1/2*H*-tetrazole compounds have been known to 'precipitate' out Ag^+ from a solution efficiently.[11] The resulting insoluble tetrazole-silver complexes are infinite metal-coordination polymers, with silver atoms binding in mono-, bi- or tri-dentate formats to the *N* atoms of the tetrazole ring.[11] For **TPE-4TA**, the anion tetrazolate acts as Ag^+-specific targeting group to trigger aggregation, while the core tetraphenylethene (TPE) endows aggregation-induced fluorescence (Fig. 1b).

TPA-4TA (X=H) was synthesized in a 21% total yield over three steps (Fig. S1). **TPA-4TA** (X=H) showed modest solubility (~10^{-4} M) in DI-water and was highly aqueous soluble (>0.05 M) when formulated in the salt form (X=Na^+).

When molecularly dissolved in aqueous solution, **TPE-4TA** is non-fluorescent, attributing to free rotational motions of phenyl rings which activated non-radioactive pathways.[9] As expected, the addition of Ag^+ lighted up a fluorescence peaked at 490–530 nm by 368 nm excitation. The turn-on response was instant. A stoichiometric study indicated that the fluorescence increased by the step-wise addition of Ag^+ (Fig. 2a). By plotting the intensity at 504 nm against the [Ag^+]/[TPE-4TA] ratio, a linear relationship with R^2 = 0.996 was established in the range of 40–15000 nM for [Ag^+] (Fig. 2b). With a further increase of [Ag^+], the fluorescence reached a steady plateau. To be noticed the linearity and the 1:1 mole ratio of Ag^+ to the tetrazolate group on approaching the plateau indicated that the sensing process correlated well with a stoichiometric metal-organic coordination-driven assembly.[12] The limit of detection for Ag^+ was estimated to be 2.3 nM, i.e., 0.25 μg/L (S/N = 3, n = 12), which is about 40 times better than the colorimetric method using dithizone (10 μg/L), and is amongst that of the best fluorescence-based methods.[13]

The fluorogenic sensing was accompanied by formation of nano-sized aggregates. The dynamic light scattering (DLS) analysis suggested that aggregates were formed with a good batch-to-batch reproducibility in solutions and the size distributions varied with the mole ratio of **TPE-4TA** to Ag^+ (Table. S1). As an example, the mixture ([TPE-4TA], 5 μM; [$AgNO_3$], 25 μM) gave a size of efficient diameter ~50 nm (Fig. 2c). After evaporation of the solvent, nano-sized particles (*d* = 5–30 nm) were also observed under electron microscopy (Fig. 2d and Fig. S4). Element mapping confirmed the clustered nanoaggregates consisting of Ag, N and C atoms (Fig. S6). The fluorescent aggregates ([TPE-4TA], 5 μM; [Ag^+], 1–50 μM) had a negative zeta potential of -15 to -40 mV, likely due to the anionic tetrazolate groups of **TPE-4TA** being exposed at the aggregate-solution interface. The colloid gave no noticeable precipitation on-shelf for over three months. The aggregates are hardly re-dissolved in common solvents, including DMSO, even at reflux conditions, likely attributing to the strong tetrazolate-silver interactions. These results supported a good colloidal stability of these fluorescent aggregates.

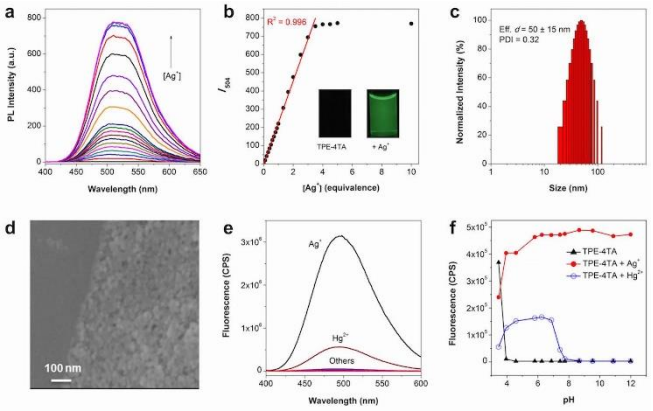

Figure 2. Characterization of the fluorogenic aggregation process. (a) Fluorescence of **TPE-4TA** (5 μM) by stepwise addition of Ag^+ in DI-water; (b) Plot of intensity at 504 nm in (a) as a function of [Ag^+]/[TPE-4TA]; (c) DLS and (d) SEM characterization of the fluorescent solution; (e) Fluorescence of **TPE-4TA** (5 μM) mixed with metal ions (20 μM, including Na^+, K^+, Ca^{2+}, Mg^{2+}, Mn^{2+}, Zn^{2+}, Cu^{2+}, Fe^{2+} Fe^{3+}, Ni^{2+}, Au^+, Pb^{2+}, Cd^{2+}, Pd^{2+} and Co^{2+}) in phosphate aqueous solution (pH 7.4); (f) Fluorescence of **TPE-4TA** (10 μM) at 504 nm against the pH values of the phosphate aqueous solution in the absence or presence of Ag^+ or Hg^{2+} (10 equiv.) respectively. Excitation: 368 nm.

The fluorogenic Ag^+ detection was next evaluated in the presense of interfering factors including different metal ions, pH, and common silver-binding reagents. Most metal ions cannot turn on the fluorescence of **TPE-4TA** (Fig. 2e and Fig. S7). Hg^{2+} lighted up a weak fluorescent signal, which may result from a similar Hg^{2+}-tetrazolate coordination.[11b] The Ag^+/Hg^{2+} coordination-induced fluorogenic detection were then evaluated at different pH values (Fig. 2f). At pH≤4, the tetrazole moiety of a pKa 4–5 was mainly in the protonated form.[14] The protonated **TPE-4TA** likely aggregated in aqueous solution and thus elicited blue emission peaked at 470 nm. At pH≥5, the probe was fully dissolved and gave a dark background. The Ag^+-induced fluorescence thus became significant. At pH>6, the maximum turn-on response kept at a stable level, indicating that it offered a robust Ag^+ quantification method from neutral to highly basic solutions. In the case of Hg^{2+} detection, the fluorogenic response was only observed within pH 5–8.

The interference tests included reagents used in silver stains and amino acids which are reported to host Ag^+ in the in-gel staining of proteins (Fig. S8). All of these interfering reagents did not trigger the fluorescence turn-on of **TPE-4TA**. When Ag^+ were bound to the reagents beforehand, **TPE-4TA** molecules were also able to snatch off (or co-aggregated with) Ag^+ from all the pre-formed Ag^+-bounded complexes included in the test and lighted up, except Ag^+-bounded cysteine complexes, likely due to the strong thiol-Ag^+ bonding.[7] The results suggested the feasibility to combine the Ag^+ sensing with biological silver staining methods.

Following the flow chart in Fig. 3a, we achieved an efficient fluorescent silver staining of proteins after SDS polyacrylamide gel electrophoresis (SDS-PAGE). For comparison, gels were also stained by conventional silver nitrate stain[8] or SYPRO Ruby fluorescent stain.[15] In the tests, a commercialized protein ladder consisting of 14 proteins served as a library of samples. In the fluorescent silver-AIE stain, all the protein bands were clearly visible under a UV lamp, correlating well with the bands stained

10.1002/anie.201801653

by SYPRO Ruby dye (Fig. 3b). The strong green color also correlated well with that of the Ag^+-probe complexes (Fig. S9). These results support that the silver-AIE stain does work in the way proposed.

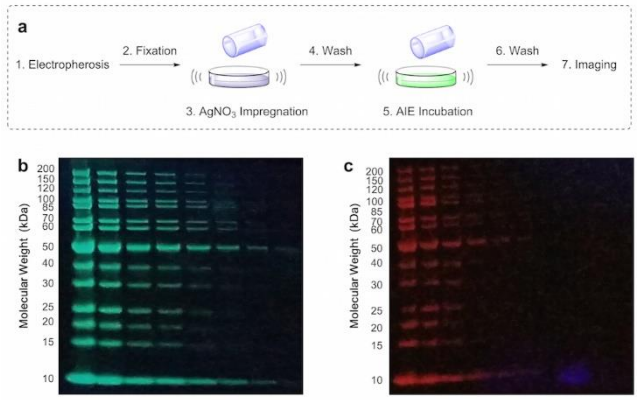

Figure 3. The fluorescent silver-AIE stain: procedure and gel images. (a) The flow chart; (b) A gel stained by the silver-AIE stain; (c) A gel stained by a SYPRO Ruby stain. (b) and (c) are imaged in parallel under 365 nm irradiation.

To compare the three staining methods, gels were analyzed by a gel imaging system (Fig. S10). Fig. 4a showed representative images, indicating that the silver-AIE stain gave a cleaner background than the silver nitrate stain and displayed a high contrast comparable to the SYPRO Ruby stain. Fig. 4b summarized their lower limit of detection (LLD), a criteria representing the sensitivity of protein detection. The silver nitrate stain gave faintly gray bands with a LLD of about 1–10 ng/band as reported.[8] The silver-AIE stain showed a high resolution and in general could detect 0–4 more lanes, i.e., 1–16 times lower LLD, than the silver nitrate stain. The sensitivity is also 1–8 times better than that of SYPRO Ruby stain. The detection is with improved performance for 10–40 kDa protein bands, indicating its advantages in low molecular weight proteins staining.

Regarding the differential protein detection, the signal profile of the 5th lane (10–25 ng/band) was shown as an example in Fig. 4c. In contrast to the silver nitrate stain which gave weak and distorted peaks, the silver-AIE stain detected all the protein bands with a good profile contrast comparable to the SYPRO Ruby stain. Since these bands showed fluorescence with comparable intensity and uniformity (Fig. 4d), the silver-AIE stain can be regarded to have minor inter-protein variation which is practically useful for total protein detection.

To compare the linear dynamic range (LDR) of the stains, we plotted the signal intensity against the amount of proteins for each band (Fig. 4d and Fig. S11). The silver-AIE stain gave a good and uniform linearity (similar slope) for all 14 proteins over a relatively broad range (Table S2). For example, for the band 8 protein, in comparison with silver nitrate stain which gave a LDR of ~1.5 logs (R^2 = 0.819), the silver-AIE stain displayed a linear range from (0.024–0.061 ng/band) to (50–75 ng/band), i.e., a LDR of over 3.3 logs (Fig. 4e). The linearity (R^2 = 0.960) is comparable with that of the SYPRO Ruby stain [R^2 = 0.957, LDR: from (0.78–1.96 ng/band) to (50–75 ng/band)], indicating that the silver-AIE stain can be used for protein quantification studies in which conventional silver stains were not recommended.[6]

The silver-AIE staining method on basis of the highly sensitive fluorogenic visualization demonstrated to be robust with low run-to-run variation. In the stain, the soluble **TPE-4TA** with AIE properties is non-emissive before developing and thus offered a low staining background. In the contrast, the control stains required lengthy destaining steps and careful timing to prevent over-staining and ensure the maximum sensitivity. In addition, the silver-AIE stain avoids the use of aldehydes which are irritant and carcinogenic, and therefore it is safer than classic silver stains.

In conclusion, we report a new water-soluble fluorogenic Ag^+ probe **TPE-4TA**, which enables the first practical fluorescent-silver staining method. **TPE-4TA** is a sensitive, selective and quantitative fluorescence turn-on Ag^+ probe and the detection works well in aqueous solutions. The coordination of anionic tetrazolate groups in **TPE-4TA** with Ag^+ results in spontaneous aggregation, which meanwhile induces turn-on fluorescence of the AIE-active probe. The fluorogenic aggregation was integrated with biological silver stains, leading to an efficient and robust fluorescent silver staining method for in-gel protein detection. With a simple and straightforward protocol, the stain achieved up to 1–16 times improvement in sensitivity compared with conventional silver nitrate stain and the famous SPRYO Ruby stain, and showed good linearity over a range of >3.3 logs for protein quantification. The novel silver staining may open a new avenue to revitalize the rich silver-based biological techniques for the study of many other argyrophilic biological structures by fluorescent methods.

Acknowledgements

This work was partially supported by the Innovation and Technology Commission (Grant No. ITC-CNERC14SC01), the University Grants Committee of Hong Kong (Grant No. AoE/P-03/08), and the Research Grants Council of Hong Kong (Grant Nos. 16301614, 16305015, N_HKUST604/14 and A-HKUST605/16). B.Z.T is also grateful for the support from The National Science Foundation of China (21788102). S. X. is grateful for the support from the Swedish Research Council (Grant No. 2017-06344).

Keywords: silver staining • protein detection • metal ion sensor • tetrazolate-silver assembly • aggregation-induced emission

10.1002/anie.201801653

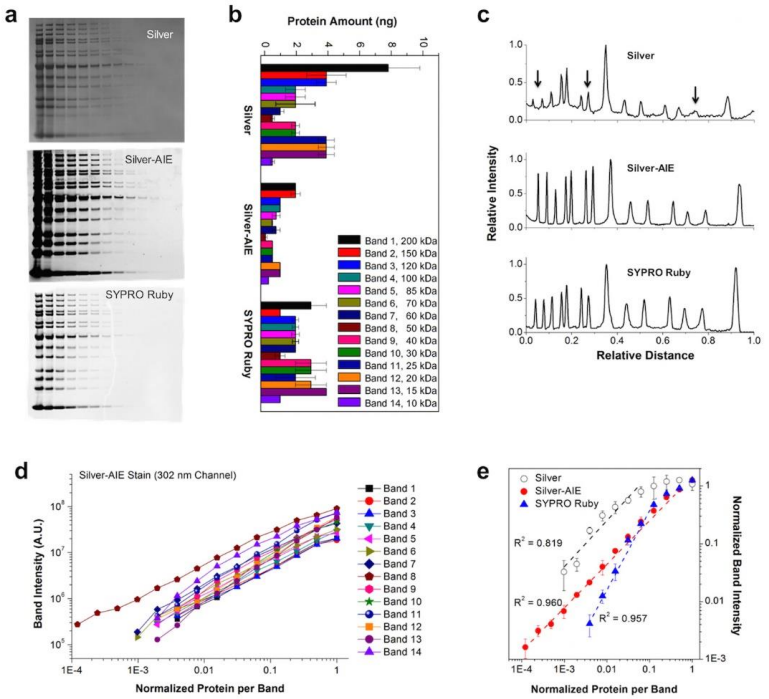

Figure 4. Comparison of the silver nitrate, fluorescent silver-AIE, and SYPRO Ruby staining methods. (a) Representative gel images. In the lanes from left-to-right, serial dilutions of ladder proteins were loaded from 200–500 ng (1st lane) to 0.012–0.003 ng (15th lane) by a factor of 2. (b) Lower limit of detection (n=3). (c) Signal profiles of the 5th lane (10–25 ng/band) showing the differential protein detection. (d) Signal intensity against the protein amount by the silver-AIE stain (n=3). (e) Signal intensity as a function of protein quantity for the band 8 protein (n=3), showing LDR of three methods. R^2: linearity of fitting lines. X-axis: value 1 equals 200–500 ng/band.

[1] G. Grant, *Brain Res. Rev.* **2007**, *55*, 490-498.

[2] T. Uchihara, *Acta Neuropathol.* **2007**, *113*, 483-499.

[3] a) R. G. Grocott, *Am. J. Clin. Pathol.* **1955**, *25*, 975-979; b) G. W. Procop, S. Haddad, J. Quinn, M. L. Wilson, N. G. Henshaw, L. B. Reller, R. L. Artymyshyn, M. T. Katanik, M. P. Weinstein, *J. Clin. Microbiol.* **2004**, *42*, 3333-3335.

[4] a) C. Goodpasture, S. E. Bloom, *Chromosoma* **1975**, *53*, 37-50; b) G. V. Sowmya, P. Nahar, M. Astekar, H. Agarwal, M. P. Singh, *Biotech. Histochem.* **2017**, *92*, 115-121.

[5] a) B. J. Bassam, P. M. Gresshoff, *Nat. Protoc.* **2007**, *2*, 2649-2654;

[6] a) M. Chevallet, S. Luche, T. Rabilloud, *Nat. Protoc.* **2006**, *1*, 1852-1858; b) I. Miller, J. Crawford, E. Gianazza, *Proteomics* **2006**, *6*, 5385-5408; c) F. Chevalier, *Proteome Sci.* **2010**, *8*, 23; d) V. J. Gauci, E. P. Wright, J. R. Coorssen, *J. Chem. Biol.* **2011**, *4*, 3-29;

[7] S. Chernousova, M. Epple, *Angew. Chem. Int. Ed.* **2013**, *52*, 1636-1653.

[8] a) L. T. Jin, S. Y. Hwang, G. S. Yoo, J. K. Choi, *Electrophoresis* **2004**, *25*, 2494-2500; b) I. R. White, R. Pickford, J. Wood, J. M. Skehel, B. Gangadharan, P. Cutler, *Electrophoresis* **2004**, *25*, 3048-3054.

[9] J. Mei, N. L. Leung, R. T. Kwok, J. W. Lam, B. Z. Tang, *Chem. Rev.* **2015**, *115*, 11718-11940.

[10] a) S. J. Chen, H. Wang, Y. N. Hong, B. Z. Tang, *Mater Horiz* **2016**, *3*, 283-293; b) X. R. Wang, J. M. Hu, G. Y. Zhang, S. Y. Liu, *J. Am. Chem. Soc.* **2014**, *136*, 9890-9893.

[11] a) L. Carlucci, G. Ciani, D. M. Proserpio, *Angew. Chem. Int. Ed.* **1999**, *38*, 3488-3492; b) J. P. Zhang, Y. B. Zhang, J. B. Lin, X. M. Chen, *Chem. Rev.* **2012**, *112*, 1001-1033; c) J. H. Lee, S. Kang, J. Y. Lee, J. H. Jung, *Soft Matter* **2012**, *8*, 6557-6563.

[12] a) G. Aromi, L. A. Barrios, O. Roubeau, P. Gamez, *Coord. Chem. Rev.* **2011**, *255*, 485-546; b) T. R. Cook, Y. R. Zheng, P. J. Stang, *Chem. Rev.* **2013**, *113*, 734-777.

[13] a) S. Singha, D. Kim, H. Seo, S. W. Cho, K. H. Ahn, *Chem. Soc. Rev.* **2015**, *44*, 4367-4399; b) L. N. Neupane, E. T. Oh, H. J. Park, K. H. Lee, *Anal. Chem.* **2016**, *88*, 3333-3340; c) D. D. Tao, Q. Wang, X. S. Yan, N. Chen, Z. Li, Y. B. Jiang, *Chem. Commun.* **2016**, *53*, 255-258; d) Y. Li, H. J. Yu, G. Shao, F. Gan, *J. Photochem. Photobiol. A* **2015**, *301*, 14-19; e) N. Sinha, L. Stegemann, T. T. Tan, N. L. Doltsinis, C. A. Strassert, F. E. Hahn, *Angew. Chem. Int. Ed.* **2017**, *56*, 2785-2789.

[14] R. J. Herr, *Bioorgan Med Chem* **2002**, *10*, 3379-3393.

[15] K. Berggren, E. Chernokalskaya, T. H. Steinberg, C. Kemper, M. F. Lopez, Z. Diwu, R. P. Haugland, W. F. Patton, *Electrophoresis* **2000**, *21*, 2509-2521.

10.1002/anie.201801653

WILEY-VCH

Entry for the Table of Contents (Please choose one layout)

Layout 2:

COMMUNICATION

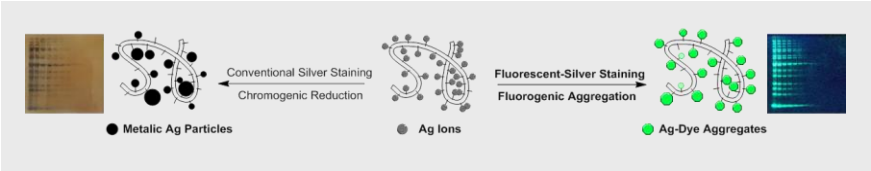

Fluorogenic development of silver: Reported is a novel fluorogenic Ag^+ detection system accomplished by a spontaneous tetrazolate-Ag^+ aggregation. This system was integrated in silver stain, substituting the tricky chromogenic reduction step of the traditional silver staining methods with a fluorogenic detection step, leading to a sensitive and robust fluorescent visualization of total proteins. This tool opens a new avenue to revitalize the rich silver-based biological techniques.

S. Xie, A. Y. H. Wong, R. T. K. Kwok, Y. Li, H. Su, J. W. Y. Lam, S. Chen, B. Z. Tang**

Page No. – Page No.

Fluorogenic Ag^+-tetrazolate Aggregation Enables Novel and Efficient Fluorescent Biological Silver Staining